Assessment of linear and non-linear EEG synchronization measures for evaluating mild epileptic signal patterns

Vangelis Sakkalis, Ciprian Doru Giurcăneanu, Petros Xanthopoulos, Michalis Zervakis, Vassilis Tsiaras, Yinghua Yang, and Sifis Micheloyannis

***Abstract*—Epilepsy is one of the most common brain disorders and may result in brain dysfunction and cognitive disturbances. Epileptic seizures usually begin in childhood without being accommodated by brain damage and many drugs produce no brain dysfunction. In this study cognitive function in mild epilepsy cases is evaluated where children with seizures are compared to controls i.e., children with epileptic seizures, without brain damage and under drug control. Two different cognitive tasks were designed and performed by both the epileptic and healthy children: i) a relatively difficult math task and ii) Fractal observation. Under this prism, we investigate seven measures of quantifying synchronous oscillatory activity based on different underlying assumptions. Namely, the most widely used coherence, a coding-based measure known as MDL (Minimum Description Length) and the Geweke alternative, a robust phase coupling measure known as PLV (Phase Locking Value), a cortical synchrony measure defined from the embedding dimension in state-space called S-estimator, a reliable way of assessing generalized synchronization also in state-space and an unbiased alternative called Synchronization likelihood. Assessment was performed in three stages; initially the methods were validated on coupled nonlinear oscillators, secondly surrogate data testing was performed to assess the possible nonlinear nature of the acquired EEGs and finally synchronization on the actual data was measured. The results on the actual data suggest higher frequency band gamma2 was mostly apparent in occipital-parietal lobes during fractal tests.**

Manuscript received June 30, 2006. This work was supported in part by the EC IST project BIOPATTERN, Contract No: 508803. The work of C.D. Giurcăneanu and Y. Yang was supported by Academy of Finland, project No. 213462 (Finnish Centre of Excellence Program 2006-2011).

V. Sakkalis is with the Department of Electronic and Computer Engineering, Technical University of Crete, Chania 73100 and the Institute of Computer Science, Foundation for Research and Technology, Heraklion 71110, Greece (+30-281-0391448; fax: +30-281-0391609; e-mail: sakkalis@ics.forth.gr).

C.D. Giurcăneanu and Y. Yang are with the Institute of Signal Processing, Tampere University of Technology, Tampere FIN-33101, Finland (e-mail: ciprian.giurcaneanu@tut.fi, yinghua yang @tut.fi).

P. Xanthopoulos and M. Zervakis are with the Department of Electronic and Computer Engineering, Technical University of Crete, Chania 73100, Greece (e-mail: petros@danai.systems.tuc.gr, michalis@systems.tuc.gr).

V. Tsiaras is with the Institute of Computer Science, Foundation for Research and Technology, Heraklion, Greece and the Department of Computer Science, University of Crete, Heraklion 71409, Greece (e-mail:tsiaras@ics.forth.gr).

S. Micheloyannis is with the Clinical Neurophysiology Laboratory (L. Widen), Faculty of Medicine, University of Crete, Heraklion 71409, Greece (e-mail: michelogj@med.uoc.gr).

I. Introduction

NEURONAL dynamics and synchronization phenomena have been increasingly recognized to be an important mechanism by which specialized cortical and sub-cortical regions integrate their activity to form distributed neuronal assemblies that function in a cooperative manner [1]. Synchronous oscillations of certain types of such assemblies in different frequency bands relate to different perceptual, motor or cognitive states and may be indicative of a wider range of cognitive functions or brain pathologies [2][3]. In general, low frequencies, like the theta band, are believed to reveal the coupling between distant brain regions, whereas high frequencies, like the gamma band, are thought to be more important for short range interactions [4].

The traditionally formulated but still the most common way of analyzing the functional coupling of cortical assemblies has been the *magnitude squared coherence (MSC)* or coherence. MSC is a normalized measure of linear dependence between two signals and is capable of identifying linear synchrony on certain frequency bands [5][6][7], but it is not able to give indications on the feedback that exists between the analyzed systems. The idea of measuring the causality between two time series can be traced back to the work of Granger [6] and Geweke [9]. The results of Geweke are especially important for neuroscience to evaluate neuronal interactions [10], because they give frequency decompositions for the time domain measures. The latter method relies on strong assumptions for the autoregressive representation of the analyzed signals, whereas the application of *Minimum Description Length principle (MDL)* relaxes these assumptions and new measures of feedback may also be introduced [11].

Since all the measures mentioned above are linear, we extend our investigations by considering also nonlinear measures. Phase Synchronization present a different approach in analyzing the possible nonlinear interdependencies of the EEG signal and focuses on the phases of the signals. The idea of studying the phase relationships of two neurophysiological signals is not new [12], but later studies has shown that even if the amplitudes of two coupled chaotic oscillators remain uncorrelated, their phases may synchronize [13]. A robust phase coupling measure is the *Phase Locking Value (PLV)* [14]. Finally,

another group of synchronization measures are based on the assumption that neurons are highly nonlinear devices, which in some cases show chaotic behavior [15]. Hence, the use of nonlinear measures derived from studying chaotic dynamical systems may be of interest in neurophysiology applications. Such measures belong to the Generalized Synchronization concept and are based on analyzing the interdependence between the amplitudes of the signals in a state-space reconstructed domain. In this study, we use three variants of this idea, the *S-estimator* [20], a robust measure proposed by [21][22] and the *synchronization likelihood* method [23].

The focus of this study is on investigating the differences in coupling of EEG channels in controls-normals versus children with mild epilepsy. We compare the capabilities of the proposed measures using chaotic noisy models and we investigate their use in real band-limited signals. We also compare the capabilities of both linear and nonlinear measures in revealing the coupling between EEG channels.

II. METHODS

A. Test Signals & Real Data Acquisition

To study the different properties of each of the proposed methods, we consider two classical coupled chaotic dynamical systems. The first model uses two coupled Rössler oscillators, whereas the second uses a Lorenz system nonlinearly driven by a Rössler oscillator with such coupling coefficient that ensures GS [26][27].

The studied population consisted of twenty mild epileptic subjects and twenty controls. The EEG signals in both groups (controls and mild epileptics) were recorded from 30 cap electrodes (FP1, FP2, F7, F3, FZ, F4, F8, FT7, FC3, FCZ, FC4, FT8, T3, C3, CZ, C4, T4, TP7, CP3, CPZ, CP4, TP8, P3, PZ, P4, PO7, PO8, O1, OZ and O2), according to the 10/20 international system, referred to linked A1+A2 electrodes. The signals were amplified using a set of Contact Precision Instrument amplifiers, filtered on-line with a band pass between 0.1 and 200 Hz, and digitized at 400 Hz. Off-line, the recorded data were carefully reviewed for technical and biogenic artifacts, so that only artifact free epochs of eight seconds duration are investigated. The procedures used in the study had been previously approved by the University of Crete Institutional Review Board and all subjects signed a consent form after the nature of the procedures involved had been explained to them.

B. Test Description

Continuous EEGs were recorded in an electrically shielded, sound and light attenuated, room while participants sat in a reclined chair. EEG data were visually inspected for artifacts and epochs of 8 sec were chosen for analysis. We analyzed epochs at rest i.e., while each individual had the eyes fixed on a small point on the computer screen and during the two cognitive tasks. The first includes two digits number subtractions or two digits minus one digit, which is thought to be a relatively difficult mathematical task and the second consist of Fractal observation. Stimuli were presented on an LCD screen located in front of the participants. Vertical and horizontal eye movements and blinks were monitored through a bipolar montage from the supraorbital ridge and the lateral canthus.

C. Mean Squared Coherence (MSC)

Let us suppose we have two simultaneously measured discrete time series x_n and y_n, $n=1\ldots N$. The most commonly used linear synchronization method is the cross-correlation function (C_{xy}) defined as:

$$C_{xy}(\tau)=\frac{1}{\mathrm{N}-\tau}\sum_{i=1}^{N-\tau}\left(\frac{x_i-\bar{x}}{\sigma_x}\right)\left(\frac{y_{i+\tau}-\bar{y}}{\sigma_y}\right) \qquad (1)$$

where $\bar{x}$ and σ_x denote mean and variance, while τ is the time lag. MSC or simply coherence is the cross spectral density function S_{xy}, which is simply derived via the FFT of (1), normalized by their individual autospectral density functions. However, due to finite size of neural data one is able to actually estimate the true spectrum, known as periodogram, using smoothing techniques (e.g. Welch's method). Thus, MSC is calculated as:

$$\gamma_{xy}(f)=\frac{\left|\left\langle S_{xy}(f)\right\rangle\right|^2}{\left|\left\langle S_{xx}(f)\right\rangle\right|\left|\left\langle S_{yy}(f)\right\rangle\right|} \qquad (2)$$

Where $\langle\cdot\rangle$ indicates window averaging in the case of Welch's method. The estimated MSC for a given frequency f ranges between 0 (no coupling) and 1 (maximum linear interdependence).

D. Geweke feedback measure

In [9] it is defined $f_{x\to y}(\omega)$, a linear measure of feedback at frequency ω from an arbitrary time series x to another time series y. We note that x and y are assumed to be wide-sense stationary and purely nondeterministic. The interested reader can find in [9] more details on this definition and on the relationship between $f_{x\to y}(\omega)$ and the MSC.

Since the analysis of coupling between EEG channels is mainly performed in frequency bands that have a well-known biomedical significance, we use the following formula for computing the coupling in $[\omega_{inf},\omega_{sup}]\subseteq[-\pi,\pi]$:

$$F_{x,y}=\frac{1}{2\pi}\int_{\omega_{inf}}^{\omega_{sup}}\left[f_{x\to y}(\omega)+f_{y\to x}(\omega)\right]\mathrm{d}\omega. \qquad (3)$$

We consider next the steps to be followed when evaluating the expression above. Given the measurements x^n and y^n, we can resort to well-known algorithms for fitting a bivariate autoregressive model. The optimal model order $\hat{p}$ can be chosen from the pre-defined set $\{p_{min},\ldots,p_{max}\}$ by applying the MDL criterion $\hat{p}=\arg\min\left[\ln|\hat{\Sigma}_p|+4p\frac{\ln N}{N}\right]$, where

$\hat{\Sigma}_p$ is the covariance matrix for the vector of residuals. The algorithm Whittle-Wiggins-Robinson (W^2R) [16] has the advantage that the stability of the estimated AR model is guaranteed. In our experiments, we have used both the W^2R algorithm and the ARFIT algorithm [17][29]. In our settings p_{max}=50, and we observed experimentally that the results produced by W^2R and ARFIT for the same data set were similar in terms of the calculated coupling values. The integral in (3) can be computed with Monte Carlo methods. More precisely, we resorted to the use of the Matlab implementation for Sobol sequences available at [30], and the number of integration points for each frequency band was 100000.

E. An MDL measure for inter-channel coupling

The dependence between time series is recast to reflect the predictability of each of the two time series from the other, and the method can be applied for measuring the coupling between band-limited signals. We are interested on evaluating the coupling between $\tilde{x}$ and $\tilde{y}$, where $\tilde{x}$ and $\tilde{y}$ are obtained after filtering x and y with a bandpass filter whose frequency range is $[\omega_{inf},\omega_{sup}]$. *MDL* principle claims the best model to be the one which leads to the shortest possible code length for the available measurements. In the hypothesis that $\tilde{y}_1^n$ must be transmitted from an encoder to a decoder, we apply the following methodology based on the results from [11].

First coding scenario: For an arbitrary prediction order $k\in\{0,..,k_{max}\}$, we compute the predicted value $\hat{y}_t$ for $\tilde{y}_t$ based on the past samples $\tilde{y}_1^{t-1}$: $\hat{y}_t=\sum_{i=1}^{k} f_i\tilde{y}_{t-i}$. Let $\varepsilon_t=\tilde{y}_t-\hat{y}_t$ be the prediction error and $E[\varepsilon_t^2]=\varsigma_k^2$. The parameters f_i are chosen such that to minimize ς_k^2, and after quantization they are sent to the decoder as side information. Then the prediction errors ε_t, $1\le t\le n$, are also sent to the decoder. The expression of the code length for y_1^n is asymptotically given by $\frac{n}{2}\ln\varsigma_k^2+\frac{k+1}{2}\ln n$. We choose the prediction order $k^*\in\{0,..,k_{max}\}$ that minimizes the code length, and the expression of the "average code length per sample" becomes $L(\tilde{y}_t|\tilde{y}_1^{t-1})=\frac{1}{2}\ln\varsigma_{k^*}^2+\frac{k^*+1}{2}\frac{\ln n}{n}$ [11].

Second coding scenario: Assuming that the decoder has complete knowledge on the past and the present of $\tilde{x}$, the current value of $\tilde{y}$ can be predicted as $\hat{y}_t=\sum_{i=1}^{k^*} g_i\tilde{y}_{t-i}+\sum_{i=0}^{\ell} h_i\tilde{x}_{t-i}$, where $\ell\in\{0,..,k^*-1\}$. Remark that the number of samples from the past of the $\tilde{y}$ process used in the linear regression is given by k^* determined in the previous step, and also the number of $\tilde{x}$ samples used in the linear regression is limited by k^*. For each possible value of ℓ, the parameters g_i and h_i are estimated from the available measurements such that to minimize the variance $\varsigma_{k^*,\ell}^2$ of the prediction errors, and then the structure parameter ℓ^* is chosen to minimize the asymptotic code length. The expression of the code length is given by $L(\tilde{y}_t|\tilde{y}_1^{t-1},\tilde{x}_1^t)=\frac{1}{2}\ln\varsigma_{k^*,\ell^*}^2+\frac{k^*+\ell^*+1}{2}\frac{\ln n}{n}$ [11].

The savings in code length of $\tilde{y}_1^n$ due to the knowledge on $\tilde{x}_1^n$ it is a measure of dependence between the two processes that it is grounded in the MDL principle. Based on this observation, we define $\mu_{\tilde{x}\to\tilde{y}}=L(\tilde{y}_t|\tilde{y}_1^{t-1})-L(\tilde{y}_t|\tilde{y}_1^{t-1},\tilde{x}_1^t)$, and similarly $\mu_{\tilde{y}\to\tilde{x}}=L(\tilde{x}_t|\tilde{x}_1^{t-1})-L(\tilde{x}_t|\tilde{x}_1^{t-1},\tilde{y}_1^t)$. We further define the *MDL* coupling measure: $\mu_{\tilde{x},\tilde{y}}=(\mu_{\tilde{x}\to\tilde{y}}+\mu_{\tilde{y}\to\tilde{x}})/2$.

Solving the estimation problem in the first coding scenario is equivalent with estimating the coefficients of an AR model, and we apply the celebrated Levinson-Durbin algorithm [18]. In our implementation, the maximum prediction order depends on the frequency band, and it takes values between 2 and 48. The second coding scenario relies on estimating the coefficients of an ARX model for which we employ the *arx* Matlab function.

F. Phase Locking Value (PLV)

One of the mostly used phase synchronization measures is the PLV approach. It assumes that two dynamic systems may have their phases synchronized even if their amplitudes are zero correlated [19]. The PS is defined as the locking of the phases associated to each signal, such as:

$$\left|n\phi_x(t)-m\phi_y(t)\right|=const \tag{5}$$

However, in this case the phase locking ratio of *n:m*=1:1, since both signals arise from the same physiological system (i.e., the brain).

In order to estimate the instantaneous phase of our signal, we transform it using the Hilbert transform (HT), whereby the analytical signal *H(t)* is computed as:

$$H(t)=x(t)+i\tilde{x}(t) \tag{6}$$

where $\tilde{x}(t)$ is the HT of *x(t)*, defined as:

$$\tilde{x}(t)=\frac{1}{\pi}PV\int_{-\infty}^{\infty}\frac{x(t')}{t-t'}dt' \tag{7}$$

where *PV* denotes the Gauchy principal value.

The analytical signal phase is defined as:

$$\phi(t)=\arctan\frac{\tilde{x}(t)}{x(t)} \tag{8}$$

Therefore for the two signals *x(t)*, *y(t)* of equal time length

with instantaneous phases $\phi_x(t), \phi_y(t)$ respectively the PLV bivariate metric is defined given by:

$$PLV = \left| \frac{1}{N} \sum_{j=0}^{N-1} e^{i(\phi_x(j\Delta t) - \phi_y(j\Delta t))} \right| \quad (9)$$

where Δt is the sampling period and N is the sample number of each signal. PLV takes values within the [0,1] space, where 1 indicates perfect phase synchronization and 0 indicates lack of synchronization.

G. S-estimator

An alternative measure for synchronization which can be applied in both bivariate and multivariate data is the S-estimator [20]. First we perform PCA meaning that we eigendecompose the covariance matrix of the data:

$$R_{FF} = E\left\{F \cdot F^T\right\} = L\Lambda L^T \quad (10)$$

where Λ is a diagonal eigenvalue matrix and L is the corresponding eigenvector matrix. From the diagonal elements λ_i of the eigenvalue matrix Λ we compute the normalized eigenvalues λ_i' as follows:

$$\lambda_i' = \frac{\lambda_i}{tr(\Lambda)} \quad (11)$$

From the K normalized eigenvalues we compute the S-estimator:

$$S = 1 + \frac{\sum_{i=1}^{K} \lambda_i' \log(\lambda_i')}{\log(K)} \quad (12)$$

We can see from (12) that when all eigenvalues are equal to 1/K then S become zero, whereas if only one strong eigenvelue exist then S becomes maximum and equal to 1. The number of eigenvalues indicates the number of uncorrelated signals within data matrix F. In brief, when the EEG channels are combinations of many uncorrelated signals no synchronization exists. On the contrary when we have small number of uncorrelated signals all brain sources are synchronized according to these signals.

H. Robust state-space GS method (RSS-GS)

Alternatively, one may measure how neighborhoods (i.e., recurrences) in one attractor maps into the other. This idea turned out to be the most robust and reliable way of assessing the extent of GS [21][22]. First, we reconstruct delay vectors [23] out of our time series; $x_n=(x_n,\ldots,x_{n-(m-1)\tau})$ and $y_n=(y_n,\ldots,y_{n-(m-1)\tau})$, where $n=1\ldots N$, and m, τ are the embedding dimension and time lag, respectively. Let $r_{n,j}$ and $s_{n,j}$, $j=1,\ldots,k$, denote the time indices of the k nearest neighbors of x_n and y_n, respectively. For each x_n the squared mean Euclidean distance to its k neighbors is defined as:

$$R_n^{(k)}(X) = \frac{1}{k} \sum_{j=1}^{k} (x_n - x_{r_{n,j}})^2 \quad (13)$$

And the Y-conditioned squared mean Euclidean distance $R_n^{(k)}(X|Y)$ is defined by replacing the nearest neighbors by the equal time partners of the closest neighbors of y_n.

If the set of reconstructed vectors (point cloud x_n) has an average squared radius $R(X) = (1/N)\sum_{n=1}^{N} R_n^{(N-1)}(X)$, then $R_n^{(k)}(X|Y) \approx R_n^{(k)}(X) \ll R(X)$ if the systems are strongly correlated, while $R_n^{(k)}(X|Y) \approx R(X) \gg R_n^{(k)}(X)$ if they are independent. Hence, an interdependence measure is defined as [21]:

$$S^{(k)}(X|Y) = \frac{1}{N} \sum_{n=1}^{N} \frac{R_n^{(k)}(X)}{R_n^{(k)}(X|Y)} \quad (14)$$

Since $R_n^{(k)}(X|Y) \gg R_n^{(k)}(X)$ by construction, it is clear that S ranges between 0 (indicating independence) and 1 (indicating maximum synchronization). Another normalized and more robust version of S maybe defined as [22] and is the one actually used in this study:

$$N^{(k)}(X|Y) = \frac{1}{N} \sum_{n=1}^{N} \frac{R_n(X) - R_n^{(k)}(X|Y)}{R_n(X)} \quad (15)$$

I. Synchronization Likelihood (SL)

Finally, the last measure (SL) used is an unbiased normalized synchronization estimator, closely related to the previous idea and to represent a normalized version of mutual information [24].

Supposing that x_n, x_v and y_n, y_v be the time delay vectors, SL actually expresses the chance that if the distance between x_n and x_v is very small, the distance between the corresponding vectors y_n and y_v in the state space will also be very small. For this, we need a small critical distance ε_x, such that when the distance between x_n and x_v is smaller than ε_x, x will be considered to be in the same state at times n and v. ε_x is chosen such that the likelihood of two randomly chosen vectors from x (or y) will be closer than ε_x (or ε_y) equals a small fixed number p_{ref}. p_{ref} is the same for x and y, but ε_x need not be equal to ε_y. Now SL between x and y at time n is defined as follows:

$$SL_n = \frac{1}{N'} \sum_{\substack{v=1 \\ w_1 < |n-v| < w_2}}^{N} \theta(\varepsilon_{y,n} - |y_n - y_v|)\theta(\varepsilon_{x,n} - |x_n - x_v|) \quad (16)$$

Here, $N'=2(w_2-w_1-1)P_{ref}$, $|\cdot|$ is the Euclidean distance and θ is the Heaviside step function, $\theta(x)=0$ if $x\leq 0$ and $\theta(x)=1$ otherwise. The value of w_1 is window equal to the Theiler correction for autocorrelation effects and w_2 is a window that sharpens the time resolution of the synchronization measure and is chosen such that $w_1 << w_2 << N$ [25]. When no synchronization exists between x and y, SL_n will be equal to the likelihood that random vectors y_n and y_v are closer than ε_y; thus $SL_n=p_{ref}$. In the case of complete synchronization $SL_n=1$. Intermediate coupling is reflected by $p_{ref} < SL_n < 1$. Finally, SL is defined as the time average of the SL_n values.

In the present study, SL was computed with the following

parameter settings: $\tau=10$; $m=10$; $w_1=100$ samples; $w_2=400$ samples; $p_{ref}=0.05$.

III. Results

A. Testing using artificially generated data using chaotic oscillators under variable noise

To demonstrate that the nonlinear synchronization methods addressed in this study are sensitive to nonlinear structures in the signals under investigation we consider two classical coupled chaotic dynamical systems. The first model uses two coupled Rössler oscillators [26], whereas the second uses a Lorenz system [27] nonlinearly driven by a Rössler oscillator with coupling coefficient that ensures GS. The synchronization indexes vs. additive noise are plotted in the following figures.

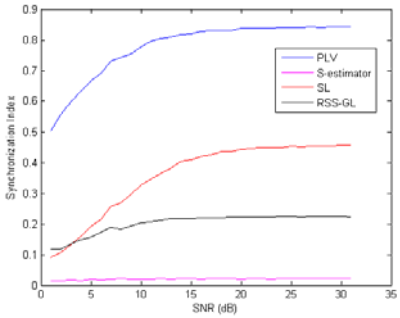

Fig. 1: Synchronization indexes applied on two coupled Rössler oscillators, configured to have phase synchronization.

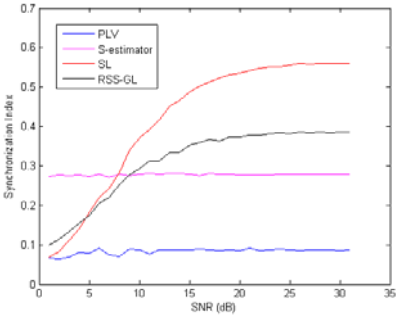

Fig. 2: Synchronization indexes applied on a Lorenz system nonlinearly driven by a Rössler oscillator. The coupling coefficient used is set for general synchronization.

B. Nonlinear coupling detection ability: Testing using surrogates

To demonstrate that the synchronization methods addressed in this study are sensitive to nonlinear structures in the real EEG signals (and thus reliable) under investigation bivariate surrogate data testing was used. The surrogating procedure used preserves both the autocorrelation of the signal and their linear cross-correlation, but the nonlinear individual structure of the individual signals, as well as their nonlinear interdependence, if any, is destroyed [28]. One mild-epileptic and one normal signal of a single representative subject was selected to be the generator of the surrogates and the testing was performed focusing on channels O2 and PO8 located on the occipital-parietal brain lobe. To reject the hypothesis (H_0) that the mean values of the original and the set of surrogate time series are equal different the Z-score is calculated. H_0 is rejected at the 95% level of confidence if Z>1.96 (one-sided test). The results obtained are tabulated below. Bold values are the ones capable of identifying the nonlinearities of the signal.

TABLE I
SYNCHRONIZATION Z-SCORES (ORIGINAL VS. SURROGATE DATASETS)

Linear (Alpha1 band, 8-10 Hz)		**Nonlinear**	
Method	**Z-score**	**Method**	**Z-score**
COHERENCE	0.50	PLV	**3.85**
GEWEKE	0.11	S-estimator	0.25
MDL	0.51	SL	1.09
		RSS-GL	1.32

C. Actual EEG data

Testing using surrogates suggested that further testing on the real data is prospective using only the linear and the *PLV* method, as discussed in the next section. The latter synchronization measures are performed on both normals and mild-epileptic band-filtered data. Averages over all possible channel couplings in each brain lobe and band are calculated (Table II). Only those bands/lobes that achieved significant differentiation using ANOVA (p=0.05) statistics

TABLE II
ACTUAL EEG DATA: LOBE-BAND SELECTION

Method	**Test1**	**Test2**	**Test3**
COHERENCE	α_1: $OPR^{(N>E)}$	-	-
GEWEKE	-	-	γ_2: $FL^{(N<E)}$
MDL	-	-	β: $OPR^{(N>E)}$ γ_2: $OPR^{(N>E)}$ γ_2: $TL^{(N>E)}$
PLV	-	-	γ_2: $CPL^{(N>E)}$ γ_2: $OPL^{(N>E)}$ γ_2: $OPR^{(N>E)}$

are tabulated. α_1, α_2, β and γ_2 denote alpha1 (8-10 Hz), alpha2 (10-13 Hz), Beta (13-30 Hz) and Gamma2 (40-90 Hz) bands, respectively. The identified lobes are: OPR (O2-P4, O2-PO8, P4-P8), OPL (O1-P3, O1-PO7, PO7-P3) and CPL (C3-CP3, CP3-P3, P3-PO7), TL (FT7-T3, T3-TP7, FT7-TP7), FL (FP1-F7, FP1-F3, F7-F3), while *N>E* denotes that synchronization in normals was greater than in epileptics.

IV. Discussion

The *PLV* method applied on phase synchronized oscillators obviously was the one performed better (Fig.1). *SL* and *RSS-GL* estimators were also able to identify the coupling, but underestimated it. *S-estimator* could not identify any PS. However on the second paradigm using the generally synchronized oscillators, all methods were able to perform well, except the *PLV* as expected (Fig. 2). *SL* and *RSS-GL* were the best, but S-estimator was very stable and

robust even in a really noisy environment. *SL* and *RSS-GL* difference responses are due to normalization factors and do not imply that one outperforms the other. As a conclusion in a real case scenario one should use both a PS measure (i.e., *PLV*) and one of the proposed GS measures (preferably *RSS-GS* or *SL*), as well as linear tools since their underlined assumptions are different.

The testing using surrogate datasets testifies that there is strong statistical evidence that the interdependence in the real EEG data can be described by a linear model, but it is also evident that there also exists nonlinear coupling apparent in PS measures (*PLV*) only. In other words, since all GS methods were unable to discriminate the actual EEG from the surrogates (linear representations), lead to the conclusion that either the actual EEG does not contain strong nonlinear GS couplings or the measure used is not strong enough to detect them. But since we tested them on nonlinear models we conclude that the first assumption is right. However, *PLV* was able to detect differences. Hence, we used *PLV* and the linear methods proposed on the real EEG data.

The results indicated that the *PLV* method accentuates gamma2 reactivity on the central and occipital brain lobes during the Fractal simulation test. Linear synchronization estimators even if they identify some additional significant brain regions, they mostly support activations around the occipital regions in gamma2 band. Such an increase in gamma band activity [33] is also found during observation of figures with illusory contours, and this finding was interpreted as an evidence of a bottom-up binding of coherent visual features [31]. At the same time, there is evidence that gamma band oscillations subserve the modulation of visual processes by the perceiver's internal representations and cognitive context, in a top-down approach [32].

REFERENCES

[1] W. Singer, "Consciousness and the binding problem," *Ann NY Acad. Sci.*, Vol. 929, pp. 123-146, 2001.

[2] E. Basar, C. Basar-Eroglu, S. Karakas, and M. Schurmann, "Gamma, alpha, delta, and theta oscillations govern cognitive processes," *Int. J. Psychophysiol*, Vol. 39, pp. 241-248, 2001.

[3] A.P. Anokhin, W. Lutzenberger, and N. Birbaumer, "Spatiotemporal organization of brain dynamics and intelligence: an EEG study in adolescents," *Int. J. Psychophysiology*, Vol. 33, pp. 259-273, 1999.

[4] A. von Stein, J. Sarnthein, "Different frequencies for different scales of cortical integration: from local gamma to long range alpha theta synchronization," *Int. J. Psychophysiol* vol. 38, pp. 301- 313, 2000.

[5] M. Ford, J. Goethe, D. Dekker, "EEG coherence and power changes during a continuous movement task," *Int. J. Psychophysiol*, vol. 4, pp. 99–110, 1986.

[6] D. Kiper, M. Knyazeva, L. Tettoni, G. Innocenti, "Visual stimulus dependent changes in interhemispheric EEG coherence in ferrets," *J. Neurophysiol*, vol. 82, issue 6, pp. 3082– 3094, 1999.

[7] S. Micheloyannis, V. Sakkalis, M. Vourkas, C.J. Stam, and P.G. Simos, "Cortical networks involved in mathematical thinking: Evidence from linear and non-linear cortical synchronization of electrical activity", *Neuroscience Letters*, Vol. 373, pp. 212-217, 2005.

[8] C.W.J. Granger, "Investigating causal relations by econometric models and cross-spectral methods," *Econometrica*, vol. 37, issue 3, pp. 424–438, 1969.

[9] J. Geweke, "Measurement of linear dependence and feedback between multiple time series," *J. of the American Statistical Association*, vol. 77, no. 378, pp. 304–313, 1982.

[10] A. Brovelli, M. Ding, A. Ledberg, Y. Chen, R. Nakamura, and S.L. Bressler, "Beta oscillations in a large-scale sensorimotor cortical network: directional influences revealed by Granger causality," *Proc. Natl. Acad. Sci. USA*, vol. 101, no. 26, pp. 9849–9854, 2004.

[11] J. Rissanen and M. Wax, "Measures of mutual and causal dependence between two time series," *IEEE Trans. on Information Theory*, vol. 33, issue 4, pp. 598–601, 1987.

[12] S.R. Butler, A. Glass, "Asymmetries in the electroencephalogram associated with cerebral dominance," *Electroencephalogr. Clin. Neurophysiol* vol. 36, issue 5, pp. 481–491, 1974.

[13] A. Pikovsky, M. Rosenblum, J. Kurths, "Synchronization: a Universal Concept in Nonlinear Science," *Cambridge University Press*, Cambridge 2001.

[14] J. Lachaux, E. Rodriguez, J. Martinerie, F. Varela, "Measuring phase synchrony in brain signals," *Hum. Brain Mapp.* vol. 8, pp. 194–208, 1999.

[15] K. Matsumoto, I. Tsuda, "Calculation of information flow rate from mutual information," *J. Phys. A,* vol. 21, pp. 1405–1414, 1988.

[16] R. Wiggins and E. Robinson, "Recursive solution to the multichannel filtering problem," *J. Geophysical Research*, vol. 70, pp. 1885-1891, 1966.

[17] T. Schneider and A. Neumaier, "Algorithm 808: ARFIT - a Matlab package for the estimation of parameters and eigenmodes of multivariate autotegressive models," *ACM Tr. Mathematical Software*, vol. 27, issue 1, pp. 58-65, 2001.

[18] P. Stoica and R.L. Moses, "Introduction to spectral analysis," *Prentice Hall, Inc*., 1997.

[19] F. Mormann, K. Lehnertz, P. David, C. Elger, "Mean phase coherence as a measure for phase synchronization and its application to the EEG of epilepsy patients," *Physica D,* vol. 144, pp. 358–369, 2000.

[20] C. Carmeli, M. G. Knyazeva, G. M. Innocenti, and O. De Feo "Assessment of EEG synchronization based on state-space analysis," NeuroImage, vol. 25, issue 2 , pp. 339-354, 2005.

[21] J. Arnhold, P. Grassberger, K. Lehnertz, C.E. Elger, "A robust method for detecting interdependencies: application to intracranially recorded EEG," *Physica D,* vol. 134 pp. 419-430, 1999.

[22] R. Quian Quiroga, A. Kraskov, T. Kreuz, P. Grassberger, "Performance of different synchronization measures in real data: a case study on electroencephalographic signals," *Phys. Rev. E,* vol. 65, no. 041903, 2002.

[23] F. Takens, D.A. Rand, L.S. Young, "Detecting strange attractors in turbulence," *Dynamical systems and Turbulence*, *Lecture Notes in Mathematics*, vol. 898, pp. 366–381, 1981.

[24] C.J. Stam, B.W. van Dijk, "Synchronization likelihood: an unbiased measure of generalized synchronization in multivariate data sets," *Physica D,* vol. 163, pp. 236–251, 2002.

[25] J. Theiler, "Spurious dimension from correlation algorithms applied to limited time-series data," *Phys. Rev. A,* vol. 34, no. 2427, 1986.

[26] A. Hramov, and A. Koronovskii "Intermittent generalized synchronization in unidirectionally coupled chaotic oscillators," *Europhysics Letters,* vol. 70, issue 2, pp. 169-175, 2005.

[27] A. Hramov and A. Koronovskii "Generalized synchronization: a modified system approach," *Physical Review E,* vol. 71, no. 067201, 2005.

[28] R.G. Andrzejak, A. Kraskov, H. Stogbauer, F. Mormann, T. Kreuz, "Bivariate surrogate techniques: necessity, strengths, and caveats," *Phys. Rev. E,* vol. 68, issue 6, no. 066202, 2003.

[29] http://www.gps.caltech.edu/~tapio/arfit/.

[30] http://www2.math.uic.edu/hanson/mcs507/cp4f04.html.

[31] C. Tallon-Baudry and O. Bertrand "Oscillatory gamma activity in humans and its role in object representation," *Trends in Cognitive Sciences*, Vol.3, pp. 151-162, 1999.

[32] V. Goffaux, A. Mouraux, S. Desmet, and B. Rossion "Human non-phase-locked gamma oscillations in experience-based perception of visual scenes," *Neuroscience Letters,* Vol. 354, pp. 14-17, 2004.

[33] S. Erimaki, et al. "EEG responses to complex fractal stimuli," *2nd International Nonlinear Sciences Conference*, Heraklion Crete, 2006.